Archives of Mining Sciences **45**, 1 (2000) 89—100

JAN KIEŁBASA *

THERMAL SENSOR OF FLOW REVERSAL

CIEPLNY INDYKATOR ODWRÓCENIA PRZEPŁYWU

The paper presents a modified theoretical description of the sensor detecting flow velocity reversal. The sensor is made of two hot, parallel wires little apart, so they can interest with one another. They lie one behind the other in the plane parallel to flow velocity. The wires are normal to the velocity vector (Fig. 1). The two wires, connected in series, are supplied from one CTA system, which means that the present sum of wire resistances remains constant. Voltage difference across the wires is the measured parameter.

Theoretical considerations lead us to the conclusion than the probe is maximally sensitive to velocities nearing zero while probe sensitivity is proportional to the distance between the wires.

Key words: thermal anemometers, hot wire anemometers, flow reversal, flow reversal detector.

W artykule przedstawiono poprawiony opis teoretyczny czujnika przeznaczonego do wykrywania zwrotu prędkości przepływu. Czujnik składa się z dwu grzanych równoległych włókien, niezbyt odległych, tak że oddziaływają cieplnie na siebie, leżących jedno za drugim w płaszczyźnie równoległej do prędkości przepływu. Włókna są do wektora prędkości prostopadłe (patrz rys. 1). Cechą charakterystyczną tego czujnika jest to, że oba włókna, połączone szeregowo, zasilane są z jednego układu stałotemperaturowego (CTA), co oznacza, że suma rezystancji obu włókien jest utrzymywana na stałym poziomie. Mierzy się różnicę napięć występujących na włóknach.

W teoretycznych rozważaniach przyjęto, że grzane włókno nie deformuje pola prędkości wokół niego, a powstający rozkład temperatury nie zmienia fizycznych stałych przepływającego medium. Można było wówczas przyjąć, że rozkład temperatury wokół dwu grzanych włókien jest superpozycją rozkładów powstających wokół pojedynczych włókien.

Otrzymano analityczne wyrażenie (57) na różnicę temperatur ΔT między włóknami. Jest ono kombinacją funkcji Bessela zerowego rzędu i funkcji hiperbolicznych od bez-

* INSTYTUT MECHANIKI GÓROTWORU, POLSKA AKADEMIA NAUK, 30-059 KRAKÓW, UL. REYMONTA 27

wymiarowych argumentów typu $v\varrho/2\kappa$, gdzie ϱ może być średnicą włókna lub odległością między włóknami. Rozwiązanie jest antysymetryczne względem prędkości przepływu, tzn. zmienia znak ze znakiem prędkości.

Rozwiązanie prowadzi do wniosku, że maksymalna czułość sondy ze względu na prędkość występuje dla zerowej prędkości i jest ona proporcjonalna do odległości między włóknami. Czułość sondy rośnie ze wzrostem nagrzania włókien.

Słowa kluczowe: anemometr cieplny, termoanemometr, indykator zwrotu przepływu, odwrócenie przepływu.

NOMENCLATURE

c — specific heat of the flowing medium at constant pressure,
l — distance between the hot wires,
r — distance between the source and the point where the measurements are taken,
r_0 — hot wire radius,
v — velocity of the flowing gas,
x — co-ordinate in the direction of the flow,
y — co-ordinate normal to the flow direction,
T_g — temperature of the flowing medium,
T_{w1} — temperature of the first hot wire,
T_{w2} — temperature of the second wire,
T_{w0} — wire temperature for the present overheating ratio n,
κ — coefficient of thermal diffusion of the flowing medium,
λ — coefficient of thermal conductivity of the flowing gas,
ϱ — density of the flowing medium.

1. Introduction

Both in theoretical considerations and in practical applications it may be necessary to measure very slow flows or detect flow reversals. We can mention here the following applications:

1. control of mine ventilation quality,
2. control of patient's breathing under narcosis,
3. providing controlled conditions (biopacks),
4. airing the hospital rooms, performance halls, storehouses, dryers, and the like,
5. control of fire sensors,
6. control of house ventilation.

A traditional hot wire anemometer, commonly applied in flow measurements, proves inadequate for these applications. First of all, its sensor will not detect flow reversals. That is obvious since the thermal losses from the hot wire, being the measure of flow velocity, are not sensitive to wire rotations round its axis. Another drawback is that its sensitivity is decreased when flow velocities are approaching zero.

Several solutions, i.e. designs of anemometers allowing for flow reversal detection can be found in literature on the subject. They mostly consist of three parallel wires [Downing 1972] where one wire is heated while the other two act as resistance thermometers. There are also two-wire options, where both wires are heated [Kiełbasa et al. 1968], [Mahler, 1972]. Several new sensors [Kiełbasa, Smolarski 1978; Kiełbasa et al. 1977, 1978; Stasicki 1983] which can be used for flow reversal detection have been engineered in the Strata Mechanics Research Institute. However, the new hot wire sensor presented in this paper seems to have most favourable parameters. The sensor consists of two thin parallel wires stretched on supports. The distance between the wires is so small that the second wire will always be in the thermal wake of the first one, therefore the temperature losses from that wire are smaller. The final effect is the asymmetry of electric resistance of these two wires. The wires considered in this paper re connected in series and incorporated in the CTA circuit, which maintains their toral resistance on constant level. Voltage difference across the wires is the measured parameter.

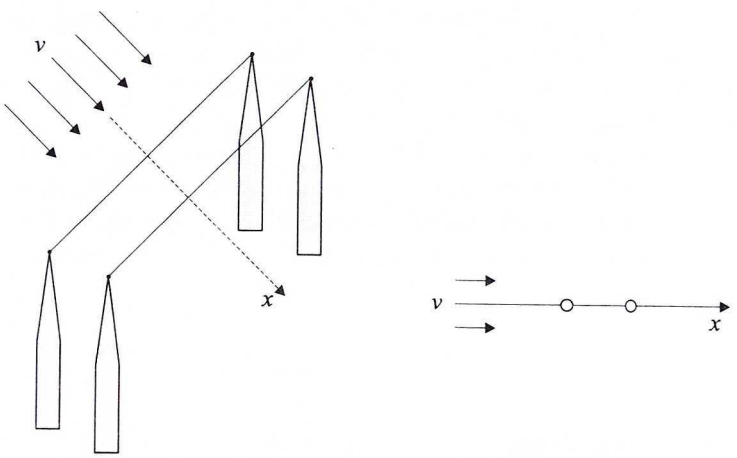

Fig. 1. Schematic diagram of a double wire sensor

2. Theoretical description

2.1. Temperature distribution around the hot wire

The physical model of such a sensor is the system of two thin, infinitely long cylinders whose axes are normal to the velocity vector and which lie in the plane parallel to this vector. The wires are connected in series and incorporated in the CTA circuit. Wire resistances are R_{w1} and R_{w2}, respectively. The electronic circuit maintains the sum of those resistances on a preset, constant level. Accordingly, we can write:

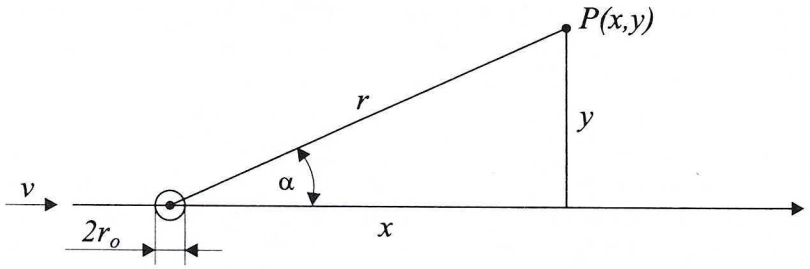

Fig. 2. Model for calculating the temperature distribution around one wire

$$R_{w1} + R_{w2} = n(R_{w01} + R_{w02}), \tag{1}$$

where: n — wire overheating ratio preset in the electronic circuit, R_{w01} — „cold" resistance of the first wire, R_{w02} — „cold" resistance of the second wire. „Cold" resistance is usually measured at the temperature of the flowing gas T_g.

The distance between the axes of the cylindrical elements is l, their diameter — $2r_0$*. The Cartesian co-ordinate system is chosen such that the x — axis coincides with flow direction, y — axis coincides with the cylinder axis and is normal to the plane $x-z$. Temperature of incoming gas at some distance from the hot wires equals T_g.

It is assumed that the presence of hot wires will not interfere with the flow**, while power imparted to the medium is so small that its physical properties will not change. In the steady state the temperature excess $T(x, y)$ at the point (x, y) above the temperature T_g around one of the cylinders (Fig. 2) determines the thermal conductivity equation (2):

$$\varrho c v \frac{\partial T}{\partial x} = \lambda \left(\frac{\partial^2 T}{\partial x^2} + \frac{\partial^2 T}{\partial y^2} \right) \tag{2}$$

with its boundary conditions:

$$T(r_0) = T_{w0} \tag{3}$$

$$\lim_{r \to \infty} T(r) = 0 \quad \text{where} \quad r = \sqrt{x^2 + y^2} \tag{4}$$

where: ϱ — density of the flowing medium, c — specific heat of the flowing medium at constant pressure, λ — coefficient of thermal conductivity of the flowing gas, v — velocity of the fluid, r_0 — hot wire radius.

---

* Thermal anemometry makes use of very thin wires, 3—20 μm in diameter.

** Presence of wires in the flow will always disturb the velocity distribution ahead of the wire; however these disturbances will vanish shortly. Experimental tests [though run on models with much larger diameters] show that the wake of the cylinder disappears at the distance equal to less than 100 diameters.

Following the transformation:

$$T(x, y) = \theta(x, y)\, e^{\alpha x} \tag{5}$$

we get:

$$\frac{\partial T}{\partial x} = \left(\frac{\partial \theta}{\partial x} + \alpha\theta\right) e^{\alpha x}, \tag{6}$$

$$\frac{\partial^2 T}{\partial x^2} = \left(\frac{\partial^2 \theta}{\partial x^2} + \frac{\partial \theta}{\partial x}\right) e^{\alpha x} + \alpha\left(\frac{\partial \theta}{\partial x} + \alpha\theta\right) e^{\alpha x} = \left(\frac{\partial^2 \theta}{\partial x^2} + 2\,\alpha \frac{\partial \theta}{\partial x} + \alpha^2 \theta\right) e^{\alpha x}, \tag{7}$$

$$\frac{\partial^2 T}{\partial y^2} = \left(\frac{\partial^2 \theta}{\partial y^2}\right) e^{\alpha x}. \tag{8}$$

Introducing (5—8) into Eq. (2), we get:

$$\frac{\partial \theta}{\partial x}(\varrho c v - 2\,\alpha\lambda) = \lambda\left(\frac{\partial^2 \theta}{\partial x^2} + \frac{\partial^2 \theta}{\partial y^2}\right) + \lambda(\alpha - \varrho c v)\,\theta \tag{9}$$

When:

$$\alpha = \frac{\varrho c v}{2\,\lambda} = \frac{v}{2\kappa} = h \tag{10}$$

then the expression containing the first derivative equals zero, accordingly Eq. (8) can be rewritten as:

$$\left(\frac{\partial^2 \theta}{\partial x^2} + \frac{\partial^2 \theta}{\partial y^2}\right) = h^2 \theta \tag{11}$$

Boundary conditions given in (3) and (4) are as follows:

$$\theta(r_0) = T_w e^{-\frac{v r_0 \cos\phi}{2\kappa}} = T_w e^{-h r_0 \cos\phi}, \tag{12}$$

$$\lim \theta(r)\big|_{r \to \infty} = 0. \tag{13}$$

Rewriting Eq. (11) in the polar coordinate system, we get:

$$\frac{\partial^2 \theta}{\partial r^2} + \frac{1}{r}\frac{\partial \theta}{\partial r} + \frac{1}{r^2}\frac{\partial^2 \theta}{\partial \phi^2} - h^2 \theta = 0, \tag{14}$$

where:

$$h^2 = \frac{v^2}{4\,\kappa^2}$$

The solution to Eq. (14) is in the form of a series:

$$\theta(r, \phi) = \sum_{n=0}^{\infty} a_n \cos(n\phi)\, K_n(|hr|). \tag{15}$$

We have to bear in mind that $|hr| = \sqrt{h^2 r^2}$, even if it is not indicated. In the further sections we will make use of the identity:

$$e^{r\cos\psi} = I_0(r) + 2\sum_{m=1}^{\infty}(-1)^m I_m(r)\cos(m\psi), \tag{16}$$

Accordingly, the boundary condition (12) can be rewritten as:

$$\theta(r_0) = T_w\left(I_0(hr_0) + 2\sum_{m=1}^{\infty}(-1)^m I_m(hr_0)\cos(m\phi)\right). \tag{17}$$

As the solution (15) must be valid for $r = r_0$, we can write:

$$\theta(r_0) = a_0 K_0(hr_0) + \sum_{n=1}^{\infty} a_n \cos(n\phi) K_n(hr_0). \tag{18}$$

Comparing the relevant coefficients we get:

$$a_0 = T_w \frac{I_0(hr_0)}{K_0(hr_0)}. \tag{19}$$

$$a_n = 2(-1)^n T_w \frac{I_n(hr_0)}{K_n(hr_0)}. \tag{20}$$

Applying (19) and (20), the solution to Eq. (2) can be rewritten as:

$$T(r,\phi) = T_w e^{r\cos\phi}\left(\frac{I_0(hr_0)}{K_0(hr_0)}K_0(hr) + 2\sum_{n=1}^{\infty}(-1)^n \frac{I_n(hr_0)}{K_n(hr_0)}K_n(hr)\cos(n\phi)\right). \tag{21}$$

This solution yields the temperature at the point defined by the radius r and the angle ϕ produced by the hot wire located at the point (0, 0) which is taken to have a surface area for the temperature T_w. Functions $I_z(z)$ and $K_n(z)$ are modified Bessel's functions of the n-th order. Let us introduce the notation:

$$w_0(r) = \frac{I_0(hr_0)K(hr)}{K_0(hr_0)}, \tag{22}$$

$$w_n(r,\alpha) = 2(-1)^n \frac{I_n(hr_0)K_n(hr)}{K_n(hr_0)}\cos n\alpha, \tag{23}$$

Accordingly, the quantity in brackets in (21) can be rewritten as:

$$w(r,\alpha) = w_0(r) + \sum_{n=1}^{\infty} w_n(r,\alpha). \tag{24}$$

Numerical analysis shows that throught the whole considered range of variability of hr_0 and hr, the subsequent terms $w_n(r,\alpha)$ are rapidly approaching zero. The first term

of the series is smaller than $w_0(r)$ by about two orders of magnitude. Thus in further calculations we may consider only the function $w_0(r)$, without the risk of committing major errors:

$$w(r,\alpha) \cong w_0(r) = \frac{I_0(hr)}{K_0(hr_0)} K_0(hr). \tag{25}$$

2.2. Temperature distribution around two wires

As the equation description the temperature distribution is linear (following an assumption that a hot wire will not significantly change the properties of the medium), the temperature distribution at the point $P(x,y) = P(r_1, \alpha_1; r_2, \alpha_2)$ produced by two sources located at points (0,0) and (1, 0) ought to have the form of linear combination (see Fig. 3).

Fig. 3. Temperature at the point (x, y) is the sum of interactions from two sources.

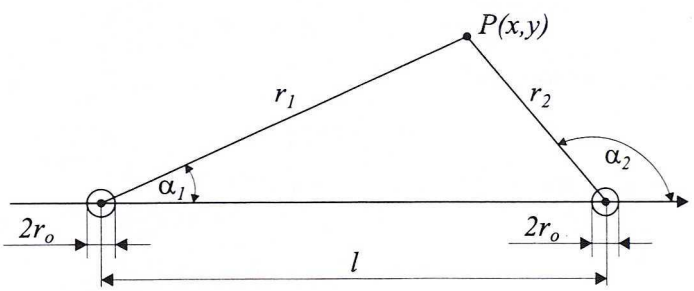

Fig. 3. Temperature at the point (x, y) being the sum of interactions from two sources

$$T(r_1, \alpha_1; r_2, \alpha_2) = T_{w1} e^{hr_1 \cos\alpha_1} w_0(r_1) + T_{w2} e^{hr_2 \cos\alpha_2} w_0(r_2) \tag{26}$$

Further considerations depend on the conditions imposed upon the hot elements. In the work of Kiełbasa and Smolarski [1978] the hot wires were connected in two independent CTA systems. In this case the situation is quite different.

2.3. Temperature wires connected into one CT system

Making use of the notation of condition (1) and rewriting is so as to reduce it to a linear relation between the resistance and temperature, we get:

$$R_{w1} = R_{w01}[1 + \gamma(T_{w1} - T_g)] \tag{27}$$

and

$$R_{w2} = R_{w02}[1 + \gamma(T_{w2} - T_g)], \tag{28}$$

Making use of the assumption:

$$R_{w01} = R_{w01} = R_{w0} \tag{29}$$

we get:

$$T_{w1} + T_{w2} = 2\frac{n-1}{\gamma}. \tag{30}$$

And analogously:

$$\Delta T = T_{w1} - T_{w2} = \frac{R_{w1} - R_{w2}}{R_{w0}}. \tag{31}$$

Making use of those formulas and assuming $\alpha_1 = 0$; $\alpha_2 = \pi$, we get:

$$T_{w1}(0, 0; l, \pi) + T_{w2}(l, 0; 0, \pi) = \frac{2(n-1)}{\gamma} \tag{32}$$

The second condition is the consequence of the requirement that the following relation should be satisfied for any v:

$$\Delta T(0, 0; l, r) = -\Delta T(l, 0; 0, \pi) \tag{33}$$

Which is equivalent to the condition:

$$\Delta T(\mathrm{v}) = -\Delta T(-v). \tag{34}$$

Making use of the solution (25), we can write:
for positive values of v

$$T_{w1}(0, 0; l, \pi) = \vartheta_1 e^{hr_0} w_0(r_0) + \vartheta_2 e^{-hl} w_0(l) \tag{35}$$

and

$$T_{w2}(l, 0; 0, \pi) = \vartheta_1 e^{hl} w_0(l) + \vartheta_2 e^{-hr_0} w_0(r_0) \tag{36}$$

for negative values of v

$$T_{w1}(0, 0; l, \pi) = \vartheta_1 e^{-hr_0} w_0(r_0) + \vartheta_2 e^{hl} w_0(l) \tag{37}$$

$$T_{w2}(l, 0; 0, \pi) = \vartheta_1 e^{-hl} w_0(l) + \vartheta_2 e^{hr_0} w_0(r_0) \tag{38}$$

The constants ϑ_1 and ϑ_2 are obtained from the conditions being imposed on anemometer operation. Since

$$\Delta T(v) = T_{w1} - T_{w2} \tag{39}$$

hence for positive values of v we get:

$$\Delta T(v) = \vartheta_1\left(\mathrm{e}^{hr_0} w_0(r_0) - e^{hl} w_0(l)\right) + \vartheta_2\left(\mathrm{e}^{-hl} w_0(l) - e^{-hr_0} w_0(r_0)\right) \tag{40}$$

Analogously, for negative values of v we get:

$$\Delta T(-v) = \vartheta_1\left(\mathrm{e}^{-hr_0} w_0(r_0) - e^{-hl} w_0(l)\right) + \vartheta_2\left(\mathrm{e}^{hl} w_0(l) - e^{hr_0} w_0(r_0)\right) \tag{41}$$

Applying (40), (41) and (34), after simple transformations we get:

$$(\vartheta_1 - \vartheta_2) = [w_0(hr_0)(e^{hr_0} + e^{-hr_0}) + w_0(hl)(e^{hl} - e^{-hl})] = 0, \tag{42}$$

This relationship should be valid for any value of v, hence

$$\vartheta_1 = \vartheta_2. \tag{43}$$

Substituting (43), (35), (36) into Eq (32), we get:

$$\vartheta_1 = \vartheta_2 = \frac{n-1}{\alpha(w_0(r_0)\cosh(hr_0) + w_0(l)\cosh(hl)} \tag{44}$$

Introducing (44) into (40) we get:

$$\Delta T = \frac{2(n-1)}{\gamma} \frac{w_0(r_0)\sinh(hr_0) + w_0(l)\sin(hl)}{w_0(r_0)\cosh(hr_0) + w_0(l)\cosh(hl)} \tag{45}$$

Making use of Eq (25), we obtain:

$$\Delta T = \frac{2(n-1)}{\gamma} \frac{K_0(hr_0)\sinh(hr_0) + K_0(hl)\sin(hl)}{K_0(hr_0)\cosh(hr_0) + K_0(hl)\cosh(hl)} = \frac{2(n-1)}{\gamma} F(r_0, l, h), \tag{46}$$

where:

$$F(r_0, l, h) = \frac{K_0(hr_0)\sinh(hr_0) + K_0(hl)\sinh(hl)}{K_0(hr_0)\cosh(hr_0) + K_0(hl)\cosh(hl)}. \tag{47}$$

Eq (47) is rather complex and difficult to analyse. It reveals that temperature difference ΔT between the two hot wires is proportional to the overheating ratio and inversely proportional to the temperature coefficient of wire resistance γ.

The behaviour of ΔT at h tending to zero or infinity is very interesting. The relevant asymptotic expansions of the present functions and asymptotic forms of (26) are given in Table. It follows from Table that the function $\Delta T(h)$ is linear for small values of h. Temperature difference is the consequence of sensor geometry, the distance 1 between the wires as well as the velocity (v) and the type of gas $\left(\kappa = \frac{\lambda}{\varrho c}\right)$. However, we must be wary while drawing conclusions concerning those asymptotic expansions, because the function ΔT given by (46) need not be monotonic.

Let us evaluate the variability range of the arguments hr_0 and hl. It is expected that the velocity v may range from -2 m/s to 2 m/s, the radius r_0 ranges from 1.5 to 5 micrometer while the distance l between the wires may range from 0.25 to 1 mm. Hence for $x_r = v_{\max} r_{\min}/2\kappa = 200$ cm/s $\times$ 0.0005 cm/(0.4 cm^2/s) = 0.25, for $x_l = v_{\max} l_{\max}/2\kappa = 200 \times 0.1/0.4 = 50$. As we can see, those arguments are far apart.

Functions $K_0(x)\sinh(x)$ and $K_0(x)\cosh(x)$ are presented in Fig. 4. It can be seen that the first function reaches its maximum for $x = 0.75$. When we sum the two

functions for the arguments hr_0 and hl, we get the first maximum for $x_0 = hl = 0.75$; the second — for $x = hr_0 = 0.75$. Bearing in mind that $h = v/2\kappa$, we can state that the maximum to the second function in the numerator in (47) will occur for the flow velocity larger that for the first function peak by l/r_0.

TABLE

Asymptonic functions present in (26)

No	Function	Asymptotic expansion for $x \to 0$	Asymptotic expansion for $x \to \infty$
1	$K_0(x)$	$-\ln(x)$	$\sqrt{\frac{\pi}{2x}e^{-x}}$
2	$\sinh(x)$	x	$\frac{e^x}{2}$
3	$\cosh(x)$	l	$\frac{e^x}{2}$
4	ΔT	$\frac{2h(n-1)}{\gamma}(l+r_0)$	$\frac{2(n-1)}{\gamma}$

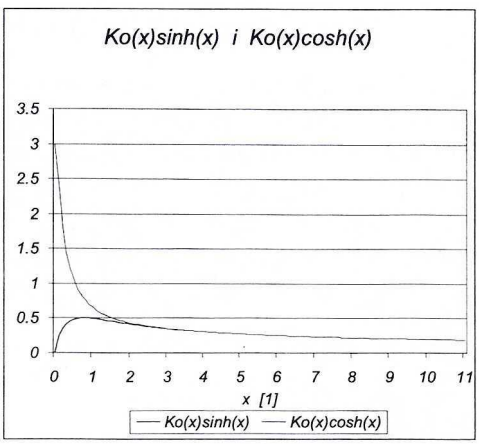

Fig. 4. Functions: $K_0(x)\sinh(x)$ and $K_0(x)\cosh(x)$

The whole term (47) is slightly different since its denominator includes the sum of products of the functions $K_0(x)$ and $\cosh(x)$. Fig 5 presents the term (47), as shown against two functions $K_0(x)\sinh(x)$, divided by 5. We can easily see that the maximum points of the function $K_0(x)\sinh(x)$ are located at the inflection points of the function (47).

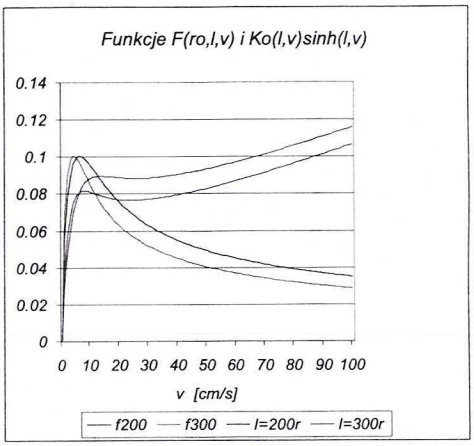

Fig. 5. Functions: $F(r_0, l, h) = \dfrac{K_0(hr_0)\sinh(hr_0) + K_0(hl)\sinh(hl)}{K_0(hr_0)\cosh(hr_0) + K_0(hl)\cosh(hl)}$ and $\dfrac{1}{5}K_0(hl)\sinh(hl)$

The function $F(r, l, h)$ has its sign changed because the function $\sinh(x)$ is asymmetric. In order to obtain the complete plot, the plot 5 should be supplemented with the function pattern in the 3rd portion of the coordinate system. This situation for the sensor consisting of a wire 5 micrometers in diameter and the distance between the wires — 100, 200, 300 and 400 times the wire radius and for velocity ranging from — 100 to 100 cm/s is represented in Fig. 6.

Temperature difference ΔT between the hot wires is proportional to the value of the function $F(r, h, l)$; accordingly its sign changes with the sign of h. That means that the sign of the velocity v determines the sign of the difference in wire resistances, and hence the sign of the voltage difference across the wires. Accordingly, the sign of the voltage difference across the wires will indicate the flow reversal within the chosen co-ordinate system.

To some extent the function ΔT depends also on the hot wire diameter. It may cause the shift of the maximum of the product of the function $K_0(hr_0)\sinh(hr_0)$ in relation to $K_0(kl)\sinh(hl)$. The final effect is that the characteristics of the function $F(r_0, l, h)$ will be raised following the first local maximum.

3. Conclusions

These considerations lead us to presume that the sensor presented in Fig. 1. supplied from a CT circuit may be used as flow reversal indicator. It displays peak sensitivity throughout the range of small velocities, nearing zero. For flow velocities which satisfy the condition

$$\left|\frac{vl}{2\kappa}\right| < 0.75$$

the sensor characteristics is monotonic and nearly linear, throughout this range. For larger velocities the sensor characteristics need not be locally monotonic, which however does not affect its function as the flow reversal indicator.

Experimental investigation of this sensor will be presented in a separate work.

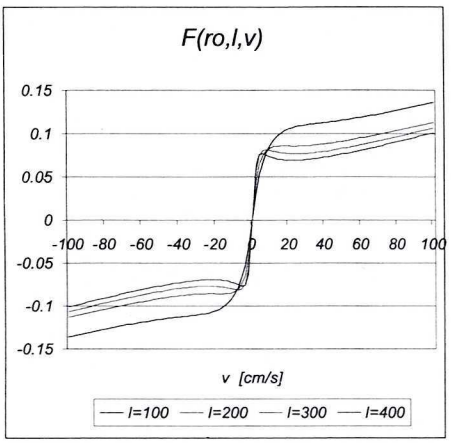

Fig. 6. Complete plots of the function $F(r_0, l, h) = \dfrac{K_0(hr_0)\sinh(hr_0) + K_0(hl)\sinh(hl)}{K_0(hr_0)\cosh(hr_0) + K_0(hl)\cosh(hl)}$

This study is a part of the research project no 8T0C00613: "Optimization of the thermal anemometer used as flow reversal indicator" supported by the State Committee for Scientific Research.

REFERENCES

Downing P. M., 1972. Reverse flow sensing hot wire anemometer. J. Phys. E5.849—851.

Kiełbasa J., Pindel Z., Rysz J., Smolarski A. Z., 1967. Anemometr elektryczny symetryczny. Patent PRL Nr 61 186.

Kiełbasa J., Pindel Z., Rysz J., Smolarski A. Z., Über einige Messmethoden der kleinen Luftgeschwindigkeiten. Proc. Of Congressus internatinalis Joachimicus de fodinarum ventilatione. 1968. A-13.

Kiełbasa J., Smolarski A. Z., Interaction of two hot-wire probes placed perpendicularly to the flow velocity vector. Bull. Acad. Pol. Sci., Ser. Sci. Techn. Vol. XXVI. Nr 10, 1978, pp. 463—469.

Kiełbasa J., Piwowarczyk J., Rysz J., Smolarski A. Z., Stasicki B., 1978. Heat waves in the metrology of flows. Proc. Of the FLOMECO 1978 IMECO — conference of Flow Measurement of Fluid — Groningen. Pp. 403—407.

Mahler D. S., 1982. Bidirectional hot-wire anemometer. Rev. Sci. Instrum. 53 (9), pp. 1465—1466.

Stasicki B., 1983. Pomiary powolnych przepływów gazów. Dysertacja doktorska. Instytut Mechaniki Górotworu PAN — Kraków.

REVIEW BY: PROF. DR HAB. INŻ. STANISŁAW DROBNIAK, CZĘSTOCHOWA

Received: 16 November 1999.